JOURNAL OF VIROLOGY, May 2004, p. 5170–5183 Vol. 78, No. 10
0022-538X/04/$08.00+0 DOI: 10.1128/JVI.78.10.5170–5183.2004

Identification of Unique Hepatitis C Virus Quasispecies in the Central Nervous System and Comparative Analysis of Internal Translational Efficiency of Brain, Liver, and Serum Variants

Daniel M. Forton,†* Peter Karayiannis,† Nadiya Mahmud, Simon D. Taylor-Robinson, and Howard C. Thomas

Hepatology Section, Division of Medicine, Faculty of Medicine, Imperial College London, London, United Kingdom

Received 6 October 2003/Accepted 9 January 2004

Reports of cerebral dysfunction in chronic hepatitis C virus (HCV) infection have led to the suggestion that HCV may infect the central nervous system (CNS). We used reverse transcription-PCR, cloning, and sequencing to define quasispecies for the HCV internal ribosomal entry site (IRES) and hypervariable region 1 (HVR1) in autopsy-derived brain, liver, lymph node, and serum samples. There was evidence of tissue compartmentalization of sequences in the brain in two patients, with between 24 and 55% of brain-derived IRES sequences absent from the serum, and significant phylogenetic and phenetic clustering of the brain and lymph node HVR1 sequences. The IRES initiates cap-independent translation of the viral polyprotein. Two unique brain-derived IRES mutations (C_{204}→A and G_{243}→A), which have previously been associated with lymphoid replication and altered translational efficiency in cell culture, were found in one patient. We used a dicistronic reporter vector to test whether brain-derived variants showed altered IRES-mediated translational efficiency, which might favor CNS infection. The translational efficiencies of the brain-derived IRES sequences were generally reduced compared to those of the master serum and liver sequences in rabbit reticulocyte cell lysates and two human cell lines, HuH7 (liver) and CHME3 (microglial). The C_{204}→A and G_{243}→A mutations showed preserved translational efficiency in HuH7 cells but reduced efficiency in CHME3 cells. Our data provide evidence that the CNS is a site of HCV replication, consistent with the recent demonstration of negative-strand HCV RNA in brain, and suggest that IRES polymorphisms may be important as a viral strategy of reduced translation to favor latency in the CNS.

The human hepatocyte is the primary locus of infection by hepatitis C virus (HCV) (14), and chronic hepatitis, cirrhosis, and hepatocellular carcinoma are the major clinical sequelae (2). However, recent reports of cerebral dysfunction in chronic HCV infection have led to the suggestion that HCV may infect the central nervous system (CNS) (9, 12, 15, 23).

Since the discovery of HCV, there have been attempts to demonstrate extrahepatic replication, most frequently in cells of haematopoietic lineage (3, 21, 26, 31, 42, 44, 59, 61, 64). These studies produced conflicting findings, as a result of methodological problems, and only recently has a consensus begun to emerge that low-level replication occurs in some extrahepatic sites, particularly in the presence of immunosuppression (4, 30, 33, 36, 43). In contrast, other members of the *Flaviviridae* family display an overt, broad cellular tropism resulting in multifaceted disease expression (60). In this context, molecular analysis of the viral genome has been useful in elucidating determinants of cellular tropism, with evidence that single amino acid substitutions in the envelope protein may alter the neurovirulence of Japanese encephalitis virus (53) and Dengue fever virus (49), both of which are members of the *Flaviviridae*.

* Corresponding author. Mailing address: Hepatology Section, Faculty of Medicine, Imperial College London, 10th Floor, QEQM Building, St. Mary's Hospital, South Wharf Rd., London W2 1NY, United Kingdom. Phone: 44 207 886 1247. Fax: 44 207 724 9369. E-mail: d.forton@imperial.ac.uk.

† D.M.F. and P.K. contributed equally to this work.

In common with a number of other positive-stranded RNA viruses within and outside the *Flaviviridae*, the 5′ untranslated region (UTR) of the HCV genome contains a highly conserved element, the internal ribosomal entry site (IRES) (5, 17, 56). This element consists of three stem-loop structures (domains II, III, and IV) and a pseudoknot and is recognized by ribosomes, thus allowing translation of the viral polyprotein in a cap-independent manner (16, 58). Although this region is the most invariant of the HCV genome, it does exhibit a quasispecies distribution in human serum (28). Naturally occurring mutations within this region are likely to be of biological significance and have been shown to lead to important differences in translation efficiency, both in cell-free systems and in cell culture (27, 28, 37, 62). Furthermore, the effect of these mutations may be to either enhance or reduce translational efficiency in different cell lines, suggesting that interactions between specific cellular factors and the IRES may be important in determining cellular tropism (27, 28, 37). A parallel may be drawn with poliovirus, where mutations within the poliovirus IRES result in reduced translational efficiency in neural but not HeLa cells, in association with a reduction in neurovirulence (25).

Several groups have reported nucleotide substitutions in the HCV IRES which are associated with lymphoid replication (33, 37, 41, 50). Long-term cultures of HCV in lymphoblastoid lines resulted in the selection of three nucleotide substitutions (G to A at position 107, C to A at position 204, and G to A at position 243) (41), which in turn increased translational activity in lymphoid cell lines (37). The same substitutions have been

TABLE 1. Clinical and virological data on the three HCV-infected patients whose autopsy tissues were studied

Patient	Gender	Diagnosis	Cause of death	HIV status	HCV genotype	Samples collected	Detection of HCV RNA in brain
A	Male	Decompensated cirrhosis, HCC[a]	Liver failure	Negative	1b	Brain, liver, lymph node, serum	Yes
B	Male	Decompensated cirrhosis	Sepsis	Negative	3a	Brain, liver, serum	Yes
C	Male	Decompensated cirrhosis, AIDS	Bacterial peritonitis	Positive	1b	Brain, liver, serum	No

[a] HCC, hepatocellular carcinoma.

found in viral sequences isolated from monocyte-derived dendritic cells (27) and peripheral blood mononuclear cells (PBMCs) (33). These results, together with the demonstration of replicative HCV intermediates in PBMCs by using highly strand-specific reverse transcription-PCR (35, 54), support the concept of HCV replication in lymphoid cells. These techniques are now being applied to study the possibility of HCV replication within the CNS. In support of CNS infection, Radkowski and colleagues recently reported the presence of negative-strand HCV RNA in autopsy brain tissue samples (48). Using single-strand conformational polymorphism, the same group showed the presence of different HCV quasispecies in brain tissue compared to serum, consistent with the presence of an independent viral compartment in the brain.

Definitive demonstration of HCV replication has proved to be challenging (14). Although assays for negative-strand RNA have been optimized and negative-strand HCV RNA has been convincingly demonstrated in cells of lymphoid origin and the CNS (35, 48, 54), the technique has previously lacked strand specificity (40, 47). It is known that negative-strand RNA degrades rapidly, with up to a 64% loss in detection after a delay of 30 min between biopsy and freezing of fresh tissue samples (38). In the context of postmortem analysis, where there is an inevitable delay in tissue availability, the sensitivity of the negative-strand assay is likely to be reduced. We therefore adopted a cloning and sequence strategy which, although labor intensive, circumvents the sensitivity and specificity issues associated with negative-strand detection. Furthermore, it is the most accurate method for analyzing quasispecies, providing information on quasispecies population parameters as well as qualitatative sequence data. In terms of the demonstration of the existence of an independent viral compartment within the CNS, this approach assumes tissue-specific evolution of HCV variants. There is considerable evidence that this occurs in the liver, PBMCs (including lymphocytes and monocytes), dendritic cells, and possibly some solid organs, particularly in immunocompromised individuals (1, 6, 32, 34, 42, 44). The possibility of tissue compartmentalization of quasispecies being due to selective adsorption of variants to cellular surfaces rather than to infection has been suggested but excluded, at least for the 5′ UTR, by adsorption studies (33).

We have previously speculated, on the basis of proton magnetic resonance spectroscopy studies, that the microglial cell might be the host cell for HCV infection within the CNS (9, 12, 55). In the present study we have tested this hypothesis by measuring the translation efficiency of brain-derived IRES sequences in a microglial cell line. We first used a cloning and sequencing strategy to define HCV quasispecies for the 5′ UTR, containing the IRES, and for hypervariable region 1 (HVR1) in brain, liver, lymph node, and serum samples collected at autopsy. The translation efficiencies of IRES variants were then tested in a dicistronic reporter vector in microglial and hepatocyte cell lines. To our knowledge, these are the first attempts to define brain-specific HCV quasispecies by sequence analysis and to determine the importance of IRES function for HCV tropism to the CNS.

MATERIALS AND METHODS

Sample collection. Tissue and serum samples were obtained at autopsy from three patients who died of complications of cirrhosis due to HCV infection (Table 1). Liver, brain (basal ganglia), serum, and in one case mesenteric lymph node tissue samples were collected within 36 h of death. The basal ganglia were selected because metabolic abnormalities have been detected in this subcortical structure in magnetic resonance spectroscopy studies of patients with HCV infection. The tissue samples were rinsed in sterile 0.7% saline and stored at −70°C until analyzed. The study was performed with institutional ethics committee approval.

RNA extraction, reverse transcription-PCR, cloning, and sequencing. RNA was extracted from 150 μg of homogenized tissue and 100 μl of serum by using a modified salt precipitation technique (Purescript; Gentra Systems, Minneapolis, Minn.). HCV RNA was reverse transcribed with Moloney murine leukemia virus reverse transcriptase (Promega, Southampton, United Kingdom), using primers from within coding regions for core and envelope protein 2 (E2) for amplification of IRES and HVR1 sequences, respectively (Table 2). Nested PCR was performed with the high-fidelity Expand system (Roche Diagnostics, East Sussex, United Kingdom) and standard and genotype-specific primers (Table 2) to amplify a 392-bp fragment encompassing the IRES and the first 42 bases of the core protein-encoding region (positions 23 to 414) and a 225-bp fragment of E2 encompassing HVR1. PCR conditions are shown in Table 2. Amplified products were gel purified (Qiaex II; Qiagen, West Sussex, United Kingdom), ligated into the pGEM-T Easy cloning vector (Promega), and transformed in competent *Escherichia coli* DH5α cells (Invitrogen, Paisley, Scotland). Between 10 and 29 clones from each sample were sequenced by the dideoxy chain terminator method with the ABI Prism 377 genetic analyzer (Perkin-Elmer, Warrington, United Kingdom).

Quasispecies analysis. Nucleotide and amino acid sequences were aligned and edited by using the DNASIS (Hitachi Software) and MEGA version 2.1 (24) programs. The 5′ UTR sequences were compared to consensus sequences to determine the viral genotype. The quasispecies complexity in each sample was expressed as Pn, which was calculated as the number of polymorphic sites divided by the number of nucleotides sequenced or amino acids. This is a measure of the variability of the sequences that comprise the quasispecies. The normalized Shannon entropy (Sn) was calculated as a measure of the size of the quasispecies repertoire and is an index of quasispecies diversity. It was calculated as $Sn = -\sum_i(p_i \ln p_i)/\ln N$, where p_i is the frequency of each sequence in the viral quasispecies and N is the total number of clones analyzed. Both Pn and Sn can theoretically vary from 0 to 1 (maximum complexity and diversity). In order to evaluate the relationships between the sequences within each compartment, distances between all possible pairs of sequences in each compartment were calculated by using the Kimura two-parameter method with a transition-to-transversion ratio of 2.0 with the MEGA package. The mean within-sample distance can be considered to be an index of the genetic spread within a compartment and a second marker of quasispecies diversity. In the case of E2/HVR1, the proportion of synonymous substitutions per potential synonymous site (*ds*) and nonsynonymous substitutions per potential nonsynonymous site (*dn*) were calculated, using the MEGA package with the Jukes-Cantor correction. Phylo-

TABLE 2. Primers used for reverse transcription and PCR amplification of HCV RNA[a]

Region	Primer set[b]	Polarity	Sequence[c]	Annealing temp (°C)
IRES	Outer	+	5′-GGGGCGACACTCCACCAT-3′	
		−	5′-GCACACCCAATCTAGGGCCCCTGCGCGG-3′ (RT)	53
	Inner	+	5′-CACTCCACCATGGATCACT-3′	
		−	5′-GGAACTTGACGTCCTGTGGGC-3′	53
	1aEcoRI (1)	+	5′-cggaattcGCCAGCCCCCTGATGGGGGCGACACTCCACCAT-3	
	3aEcoRI (3)	+	5′-cggaattcGCACCTGCCTCTTACGAGGCGACACTCCACCAT-3′	
	UEcoRI	−	5′-ctggaattcCGGGAACTTGACGTCCTGTGGGC-3′	50
E2/HVR1	Outer (1)	+	5′-GGGATATGATGATGAACTGG-3′	
		−	5′-TCCCACCACCACGGGGC-3′ (RT)	52
	Outer (3)	+	5′-GCTTGGGATATGATGATGAACTGGTC-3′	
		−	5′-GGTGTGGAGGGAGTCATTGCAGTT-3′ (RT)	60
	Inner	+	5′-CACTGGGGAGTCCTGGCG-3′	
		−	5′-CGAGTGCTGTTGATGTGCCA-3′	58

[a] PCR were carried out at the annealing temperature shown over 35 cycles.
[b] Genotype-specific primers are indicated by the genotype in parentheses. RT, primers used for reverse transcription. 1aEcoRI, 3aEcoRI, and UEcoRI are primers which were used to amplify IRES sequences of interest for the purpose of cloning into the dicistronic vector.
[c] The EcoRI restriction site and non-HCV nucleotides are indicated by lowercase.

genetic trees were constructed by the neighbor-joining method in MEGA by using the Kimura two-parameter model at the nucleotide level and p-distances at the amino acid level. Bootstrap values were determined from 500 bootstrap resamplings of the original data. Mantel's test (1, 45) was used to determine whether sequences within each extrahepatic compartment (brain, lymph node, and serum) shared more genetic identity with each other than sequences from the other extrahepatic compartments. This phenetic analysis determines the degree of genetic similarity among sequences, in contrast to phylogenetic analyses, which determine ancestral relationships among sequences. The Kimura two-parameter distance matrix is compared to a compartment distribution matrix M_C of the same dimensions, where $M_C(i,j) = 0$ if sequence i is from the same compartment as j and $M_C(i,j) = 1$ if i is from a compartment different from j. The test statistic is the square of the Pearson correlation coefficient, r^2, computed over all of the pairs of elements of both matrices. The null distribution was constructed by randomly permuting the rows and columns of M_C 5,000 times and counting the number of times that r^2 is exceeded. The hypothesis that there is no compartmental structure is rejected if fewer than 5% of the permutations exceed r^2.

Construction of the DCV dicistronic vector. HCV IRES translation efficiency was tested in a dicistronic reporter vector, DCV, consisting of two reporter genes, the *Firefly* (Fluc) and *Renilla* (Rluc) luciferases, flanking the IRES sequence. The mRNA encoding the reporter genes is transcribed under the control of the simian virus 40 promoter in cell-based systems or the T7 promoter in cell-free ones. In either case, translation of the upstream (control) reporter (Rluc) occurs by a cap-dependant mechanism, whereas translation of the downstream reporter (Fluc) is under the control of the interposed HCV IRES. In brief, the Fluc gene was amplified by PCR (30 cycles; annealing temperature, 58°C) with 10 ng of pSP-*luc*+NF (Promega) and 30 pmol each of primers FLUCF (5′-AGTCTAGACTCGAGGAATTCATGGTCACCGACGCCAAAA ACATAAAG-3′) and FLUCR (5′-TCTCTAGAATTACACGGCGATCTTTC CGCC-3′), using the Expand long-range system (Roche). FLUCF and FLUCR contain an XbaI restriction site (underlined). The PCR product was ligated into pGEM-T Easy and then digested with XbaI. The purified fragment was next ligated into pRL-SV40 (Promega) containing Rluc. This was first linearized by XbaI digestion and treated with alkaline phosphatase (Promega). This generated the dicistronic vector (DCV) consisting of the two luciferase genes separated by a unique XhoI/EcoRI cloning site (underlined in FLUCF). Selected IRES sequences of interest were amplified by PCR with 3 to 5 ng of mini-prepped DNA and genotype-specific primers (1aEcoRI, 3aEcoRI, and UEcoRI [Table 2]). The resulting amplicons included stem-loop I of the 5′ UTR, the entire IRES, and the first 42 nucleotides of the core-coding sequence, flanked by EcoRI restriction sites. These products were digested with EcoRI and ligated into EcoRI-linearized and phosphatase-treated DCV. The resulting constructs were sequenced in both directions to confirm the correct orientation of the inserted IRES fragment.

Determination of IRES quasispecies translational efficiency. In order to determine whether the observed IRES mutations were of functional importance, in vitro IRES translational efficiency was measured by using the TNT coupled rabbit reticulocyte lysate system (Promega). One microgram of each DCV-IRES construct was used per reaction mixture, and the luminometric activities of both Fluc and Rluc in the cell lysates were measured by using the dual luciferase kit (Promega) and a multiwell plate reading luminometer (Berthold Technologies, Hertfordshire, United Kingdom). The Fluc/Rluc ratio was calculated as an index of IRES translational activity. The experiments were repeated at least three times.

Two cell lines were then used to test translational efficiency following transfection of selected constructs. HuH7 cells of hepatocellular carcinoma origin and CHME3 cells of fetal microglial origin (kindly provided by N. Janabi) were maintained in Dulbecco modified Eagle's medium (Invitrogen), supplemented with 10% fetal calf serum, 2 mM L-glutamine, penicillin (100 IU/ml), and streptomycin (100 μg/ml). HuH7 cells, seeded in 24-well plates, were transfected when subconfluent with 1 to 2 μg of each DCV-IRES construct mixed with 2 μl of Lipofectin (Invitrogen) in 300 μl of Optimem (Invitrogen). Cells were lysed, at 24 h posttransfection, using 100 μl of passive lysis buffer (dual luciferase kit; Promega) per well, and luciferase activities were measured immediately as described above. The transfections were done in triplicate. A total of 2×10^9 CHME3 cells were electroporated with 6 μg of each DCV-IRES construct in a 0.4-cm cuvette (voltage, 1.5 kV/cm; capacitance, 25 μF). The electroporated cells were maintained in medium for 24 h and then lysed, and their luciferase activities were measured as described above, again in triplicate.

Mean translational activities were expressed relative to the dominant serum IRES variant, arbitrarily designated 100%, and differences were analyzed by analysis of variance, with a post-hoc Bonferroni test, using the SPSS version 10 package.

RESULTS

Compartment-specific sequences. HCV RNA was detected in brain extracts from two out of three patients (patients A and B), both of whom were human immunodeficiency virus (HIV) negative. The viral genotypes in these cases were 1b (patient A) and 3a (patient B). Totals of 167 and 117 clones were sequenced for patients A and B, respectively. In each case, characteristic quasispecies distributions were found in all samples, with the presence of a dominant sequence (master sequence) and a variable number of minority sequences (Fig. 1 to 3). With the exception of the master HVR1 nucleotide sequence in serum in patient A, the master sequences from each tissue compartment were identical in each patient. However,

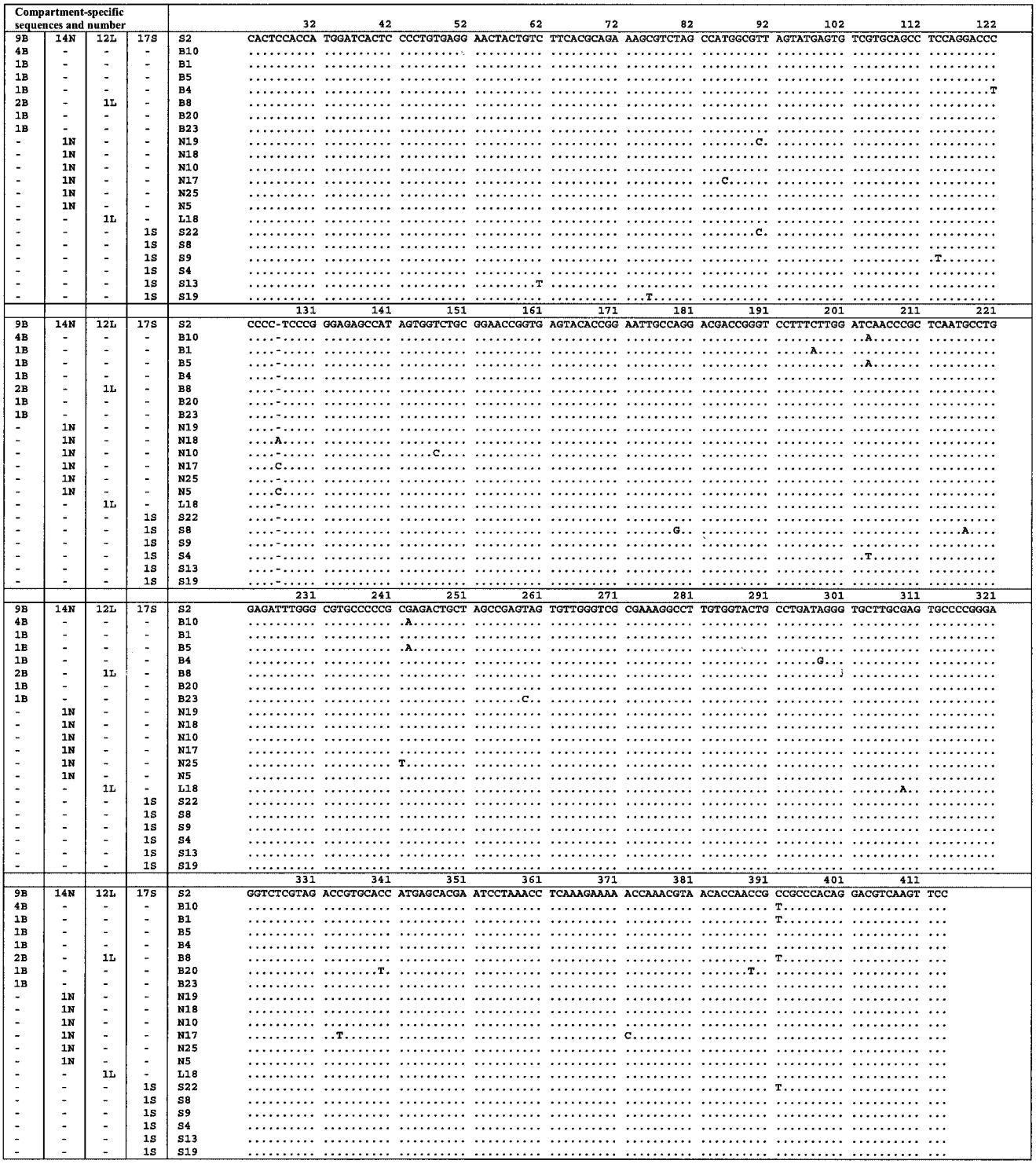

FIG. 1. Nucleotide alignment of IRES sequences amplified from brain, liver, serum, and lymph node for patient A. Sequences are compared to the master sequence, which was the same in each compartment. The numbers of sequences in each compartment are given in the four columns on the left. The identifier for each sequence is given in the fifth column. Nucleotide numbering as described by Choo et al. (7). B, brain; N, lymph node; L, liver; S, serum.

the number and distribution of minority sequences varied across the tissue compartments. As expected, the nucleotide complexity, as measured by Pn, was greater in HVR1 than in the IRES sequences, consistent with the known variability of this region (Tables 3 and 4). Similarly, the mean within-patient genetic distance was greater in the HVR1 quasispecies than in the IRES (0.02 versus 0.002 in patient A and 0.007 versus 0.002 in patient B). However, the normalized Sn was of a similar

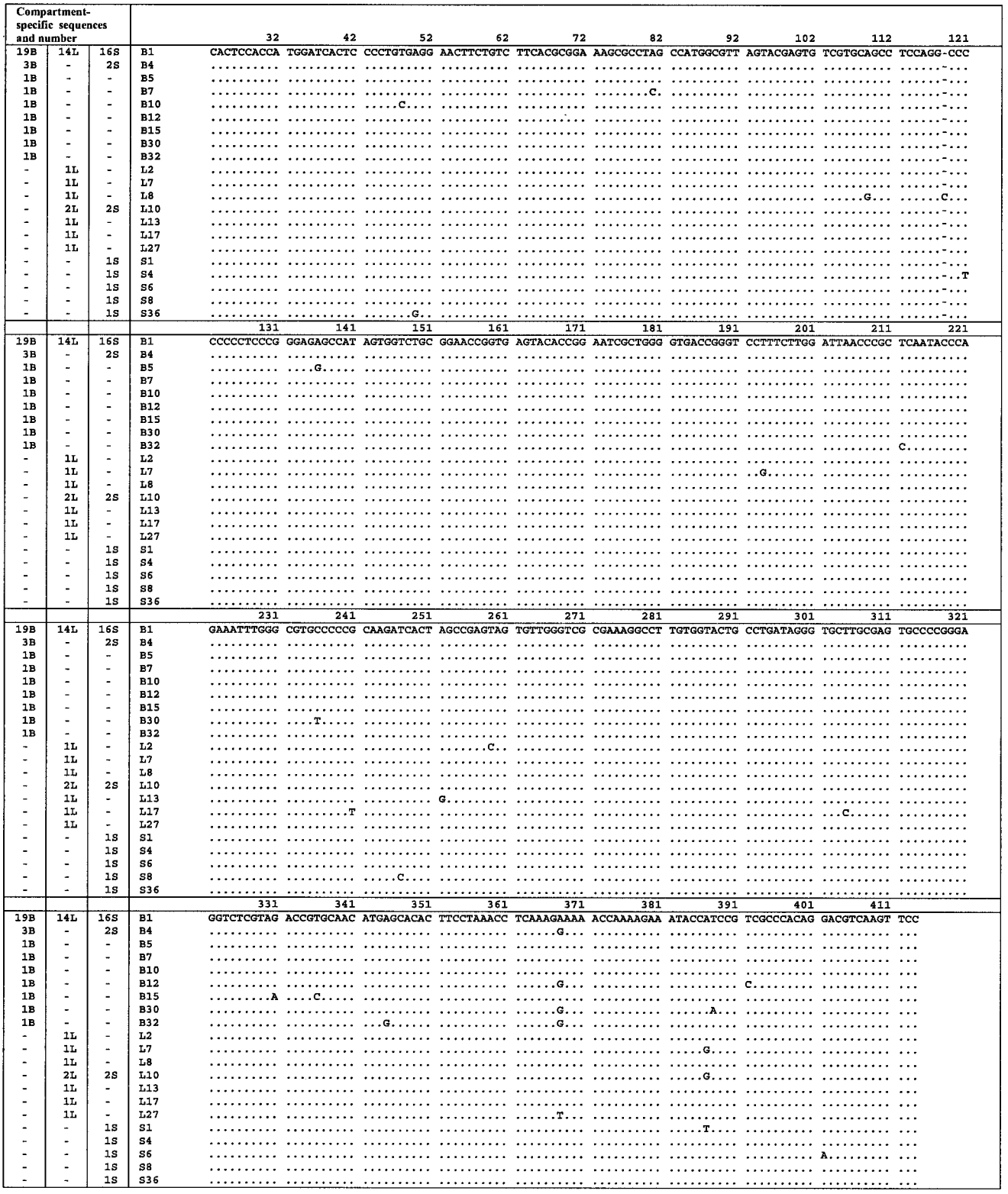

FIG. 2. Nucleotide alignment of IRES sequences amplified from brain, liver, and serum in patient B. Sequences are compared to the master sequence, which was the same in each compartment. The numbers of sequences in each compartment are given in the three columns on the left. The identifier for each sequence is given in the fourth column. B, brain; N; L, liver; S, serum.

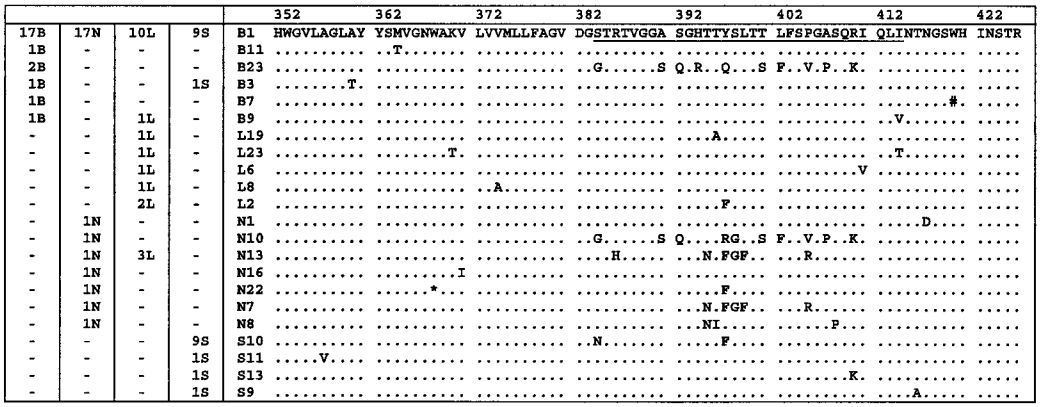

17B	17N	10L	9S		352 HWGVLAGLAY	362 YSMVGNWAKV	372 LVVMLLFAGV	382 DGSTRTVGGA	392 SGHTTYSLTT	402 LFSPGASQRI	412 QLINTNGSWH	422 INSTR
1B	-	-	-	B11	.....	..T.....	.....	.....	.....	.....	.....	.....
2B	-	-	-	B23	.....	.....	.....	..G.....S	Q.R..Q...S	F..V.P..K.	.....	.....
1B	-	-	1S	B3	.....T.	.....	.....	.....	.....	.....	.....	.....
1B	-	-	-	B7	.....	.....	.....	.....	.....	.....	.....#.	.....
1B	-	1L	-	B9	.....	.....	.....	.....	.....	.....	..V.....	.....
-	-	1L	-	L19	.....	.....	.....	.....	....A.....	.....	.....	.....
-	-	1L	-	L23	.....	.....T.	.....	.....	.....	.....	..T.....	.....
-	-	1L	-	L6	.....	.....	.....	.....	.....	V	.....	.....
-	-	1L	-	L8	.....	.....	..A.....	.....	.....	.....	.....	.....
-	-	2L	-	L2	.....	.....	.....	.....	.....F....	.....	.....	.....
-	1N	-	-	N1	.....	.....	.....	.....	.....	.....	.....D....	.....
-	1N	-	-	N10	.....	.....	.....	..G.....S	Q....RG..S	F..V.P..K.	.....	.....
-	1N	3L	-	N13	.....	.....	.....	....H.....	...N.FGF..	...R.....	.....	.....
-	1N	-	-	N16	.....	I	.....	.....	.....	.....	.....	.....
-	1N	-	-	N22	.....	.....*...	.....	.....	.....F....	.....	.....	.....
-	1N	-	-	N7	.....	.....	.....	.....	...N.FGF..	...R.....	.....	.....
-	1N	-	-	N8	.....	.....	.....	.....	...NI.....	.....P...	.....	.....
-	-	-	9S	S10	.....	.....	.....	..N.....	.....F....	.....	.....	.....
-	-	-	1S	S11	.....V....	.....	.....	.....	.....	.....	.....	.....
-	-	-	1S	S13	.....	.....	.....	.....	.....	.....K.	.....	.....
-	-	-	1S	S9	.....	.....	.....	.....	.....	.....	....A.....	.....

Patient A

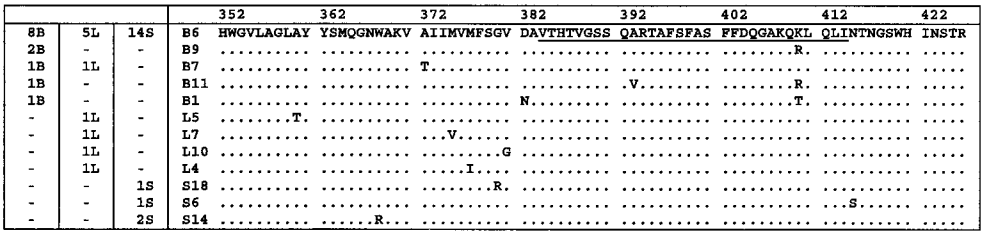

8B	5L	14S		352 HWGVLAGLAY	362 YSMQGNWAKV	372 AIIMVMFSGV	382 DAVTHTVGSS	392 QARTAFSFAS	402 FFDQGAKQKL	412 QLINTNGSWH	422 INSTR
2B	-	-	B9	.....	.....	.....	.....	.....	.....R.	.....	.....
1B	1L	-	B7	.....	.....	T.....	.....	.....	.....	.....	.....
1B	-	-	B11	.....	.....	.....	.....	.V.....	.....R.	.....	.....
1B	-	-	B1	.....	.....	.....	N.....	.....	.....T.	.....	.....
-	1L	-	L5	.....T.	.....	.....	.....	.....	.....	.....	.....
-	1L	-	L7	.....	.....	...V.....	.....	.....	.....	.....	.....
-	1L	-	L10	.....	.....	.....G	.....	.....	.....	.....	.....
-	1L	-	L4	.....	.....	.....I....	.....	.....	.....	.....	.....
-	-	1S	S18	.....	.....	.....R.	.....	.....	.....	.....	.....
-	-	1S	S6	.....	.....	.....	.....	.....	.....	...S.....	.....
-	-	2S	S14	.....	......R...	.....	.....	.....	.....	.....	.....

Patient B

FIG. 3. E2/HVR1 peptide alignments from serum and tissue compartments in patients A and B. These sequences are compared to the master sequence, which was the same in each compartment. The numbers of sequences in each compartment are given in the columns on the left. The identifier for each sequence is given before the sequence. B, brain; N, lymph node; L, liver; S, serum; *, stop codon; #, insertion of C at nucleotide position 1600. HVR1, comprising amino acids 384 to 414 is underlined in the master sequence.

order for both regions, indicating broadly similarly sized quasispecies repertoires. These findings are consistent with previous reports of a quasispecies distribution within the 5′ UTR, subject to stronger conservatory constraints than the coding regions (28, 51).

Analysis of IRES cloning and sequencing results. Between 14 and 29 IRES clones from each anatomical compartment were sequenced. The master sequences in the compartments were identical and accounted for 45 to 86% of clones (Table 3; Fig. 1 and 2); this is hereafter referred to as the consensus sequence.

In patient A, the brain had the highest number of unique clones (45%) and a majority of brain clones (55%) had sequences that were not represented in the serum quasispecies pool. The brain-derived quasispecies were more complex and diverse than those from the other compartments. This is reflected in substantially greater Sn, Pn, and mean within-sample genetic distance values ($P < 0.0001$). The serum and lymph

TABLE 3. IRES quasispecies parameters from brain, liver, and serum for patients A and B, as determined by nucleotide substitution analysis[a]

Patient	Sample	No. of clones analyzed	No. (%) of clones not seen in serum	Normalized complexity (Pn) (10^{-3})	Normalized Sn	Mean within-sample distance (10^{-3})[b]
A	Brain	20	11 (55)	1.15	0.55	4.7**
	Liver	14	2 (14)	0.36	0.19	0.7**
	Serum	23		0.88	0.38	1.8
	Lymph node	20	6 (30)	0.89	0.38	1.6
B	Brain	29	7 (24)	0.97	0.39	2.6*
	Liver	22	5 (22)	0.93	0.44	2.3
	Serum	25		0.61	0.41	1.8

[a] Lymph node quasispecies were also analyzed for patient A.

[b] The mean within-sample genetic distances were calculated by using the Kimura two-parameter method with a transition-to-transversion ratio of 2.0, using MEGA version 2.1. **, $P < 0.0001$; *, $P < 0.01$ (compared to serum).

TABLE 4. E2/HVR1 quasispecies parameters from brain, liver, and serum for patients A and B, as determined by nucleotide (nt) and amino acid (aa) substitution analysis[a]

Patient	Sample	No. of clones analyzed	No. (%) of clones not seen in serum		Normalized complexity (Pn) (10^{-2})		Normalized Sn		*ds*/*dn*[b]	Mean within-sample distance (10^{-2})[c]
			nt	aa	nt	aa	nt	aa		
A	Brain	23	23 (100)	5 (21)	0.63	0.81	0.59	0.31	3.4	2.5*
	Liver	20	20 (100)	10 (50)	0.44	0.72	0.78	0.53	1.5	1.6
	Serum	22			0.24	0.36	0.57	0.42	5.5	1.8
	Lymph node	24	24 (100)	7 (29)	0.71	0.94	0.71	0.37	2.6	2.2
B	Brain	13	9 (69)	5 (38)	0.31	0.41	0.75	0.45	3.1	0.9**
	Liver	10	5 (50)	5 (50)	0.36	0.53	0.65	0.65	2.5	0.9**
	Serum	18			0.10	0.22	0.37	0.26	1.6	0.3

[a] Lymph node quasispecies were also analyzed for patient A.
[b] Ratio of the mean proportion of synonymous mutations per synonymous site to the mean proportion of nonsynonymous mutations per nonsynonymous site, as computed by MEGA version 2.1, with the Jukes-Cantor correction.
[c] The mean within-sample genetic distances were calculated by using the Kimura two-parameter method with a transition-to-transversion ratio of 2.0, using MEGA version 2.1. **, $P < 0.0001$; *, $P = 0.04$ (compared to serum).

node quasispecies displayed comparable population parameters with intermediate complexity and diversity. In both cases unique variants were seen, although these were represented only by single clones. The liver-derived sequences were the most invariant.

In patient B, the size of the quasispecies repertoire (Sn) and the prevalence of the consensus sequence were similar across the three compartments. However, Pn and the mean within-sample distance of the brain ($P < 0.01$) and liver quasispecies were greater than those for serum, indicating that the minor strains in brain and liver were more divergent.

Phylogenetic trees constructed from the viral sequences showed a number of unique brain-derived sequences in both patients (Fig. 4). In patient A, five brain-derived clones (B5, B10, B13, B18, and B25) clustered together (bootstrap score = 75) and were phylogenetically distinct from the consensus sequence, which was present in all compartments and likely to represent serum-derived virus. These brain-derived sequences contain the substitutions C to A at position 204 and G to A at position 243 (hereafter referred to as A204, A243), which have previously been reported to be associated with extrahepatic replication (33, 37, 41, 50). In patient B, there was no phylogenetic grouping by compartmental origin. However, the minor brain variants showed the greatest evolutionary distance from the consensus sequence.

The Mantel test supported a phenetic structure to the extrahepatic compartments in patient A ($P < 0.001$), but this was not evident in patient B.

Analysis of E2/HVR1 cloning and sequencing results. Between 10 and 24 E2/HVR1 clones from each anatomical compartment were sequenced. In patient A, the brain quasispecies complexity (Pn) was broadly equivalent to that in the other tissue compartments (Table 4), in contrast to the IRES data (Table 3). Sn was greatest in the liver quasispecies, indicating the broadest quasispecies repertoire. However, the mean within-sample distance was greater in the brain ($P < 0.02$) and lymph node clones, indicating greater evolutionary distances within these compartments. This is seen clearly on the amino acid phylogenetic tree (Fig. 4), where there is significant clustering of two brain clones (B23 and B6; bootstrap value = 95). Within HVR1 (residues 384 to 410), these clones differ from the consensus sequence at 10 out of 27 amino acids and are most closely related to a lymph node clone (N10; bootstrap value = 99). At the amino acid level, there were two dominant sequences from serum, one of which was the same as the consensus sequence in the other compartments. The second dominant serum-derived sequence (S10), accounting for 41% of serum clones, was not seen in any of the tissue compartments. The Mantel test supported a phenetic structure for the extrahepatic compartments ($P < 0.001$).

In patient B the E2/HVR1 quasispecies parameters paralleled those in patient A, with greater Pn, Sn, and mean within-sample distance values in brain and liver compared to serum. Three brain clones (B5, B9, and B11) had a lysine (K)-to-arginine (R) substitution at the carboxyl end of HVR1 and clustered together on the phylogenetic tree (bootstrap value = 61). The Mantel test supported phenetic compartmentalization of the brain clones ($P = 0.006$).

In order to determine whether there were different host selection pressures acting on different anatomical compartments, *ds*/*dn* ratios were calculated (Table 4). In all cases, the *ds*/*dn* ratio was greater than 1, indicating that positive immune selection was not occurring in any compartment.

IRES translation efficiency in cell lysates. IRES sequences of interest were ligated into DCV, as described earlier, and their translational efficiencies were measured by assaying for

FIG. 4. Phylogenetic tree analyses of IRES and E2/HVR1 sequences from patients A and B. The trees representing the IRES nucleotide sequences were constructed by using the neighbor-joining algorithm and the Kimura two-parameter method in MEGA version 2.1. Trees representing the E2/HVR1 amino acid sequences were constructed by using the neighbor-joining algorithm and p-distances in MEGA version 2.1. Bootstrap values were derived from 500 resamplings of the original data. There was evidence of phenetic compartmentalization of the extrahepatic sequences where indicated (**, $P < 0.001$; *, $P < 0.01$ [Mantel test]). B, brain (●); N, lymph node (○); L, liver (▲); S, serum (□).

Patient A

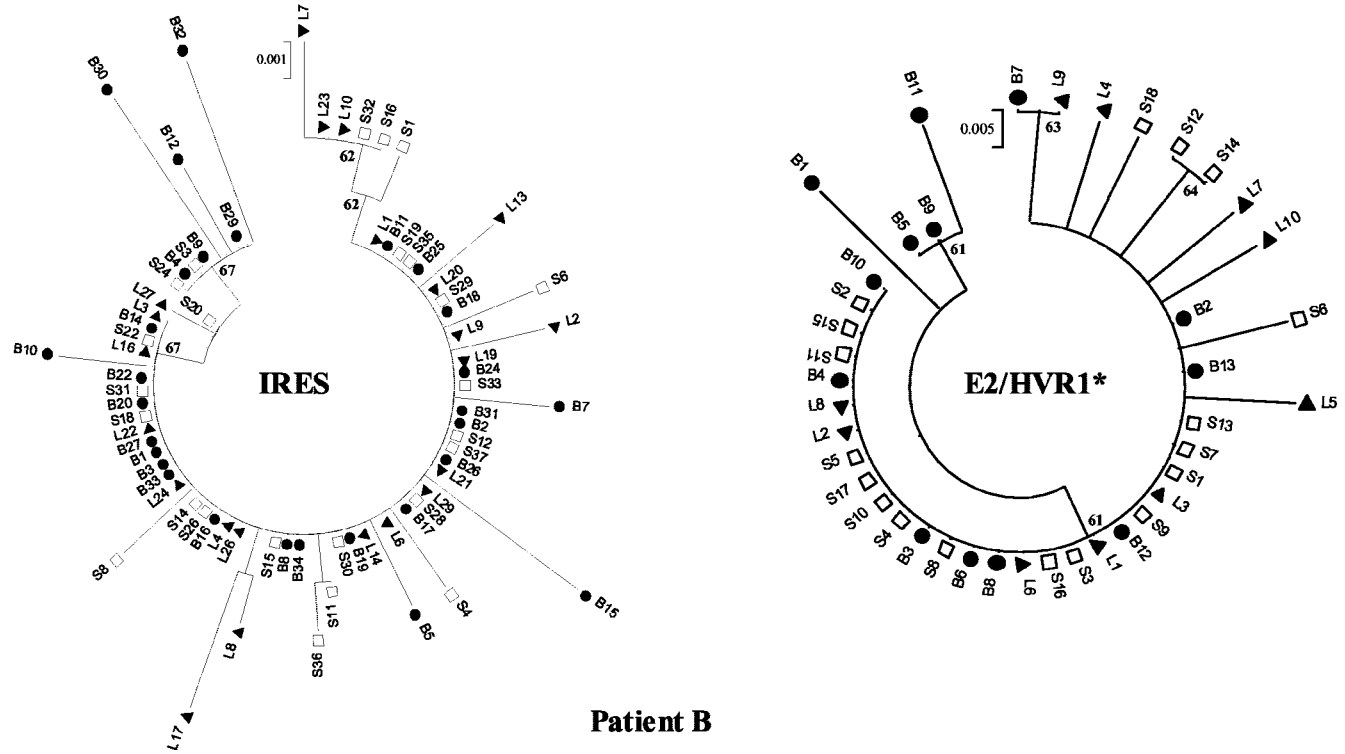

Patient B

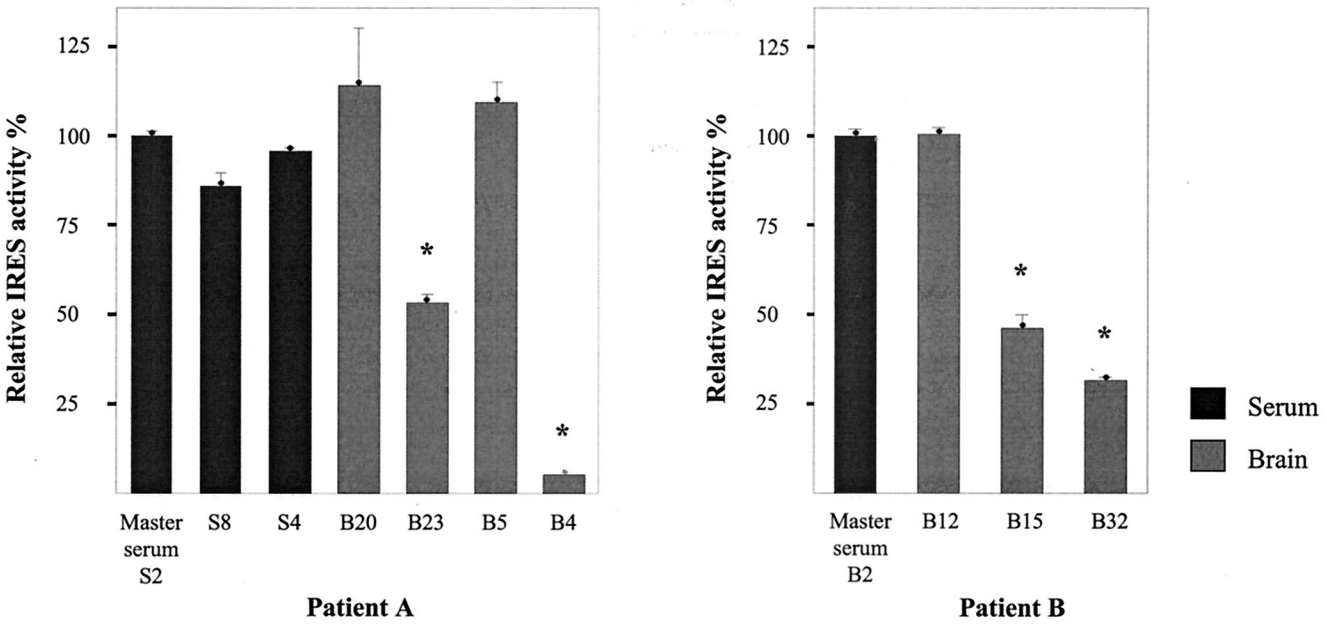

FIG. 5. Translation efficiencies of HCV IRES variants in rabbit reticulocyte cell lysates from patients A and B. Translation efficiencies are shown relative to the master serum variant. The results shown represent the means obtained from at least three experiments for each IRES ± standard errors. *, $P < 0.001$.

luciferase activity in a cell-free system. In both patients, the consensus sequence showed the highest translational efficiency (Fig. 5). In patient A, two brain-derived sequences (B4 and B23) showed marked reductions in IRES function compared to the consensus sequence (translational activity for B4 = 5%, and translational activity for B23 = 53% [$P < 0.001$]). B4 contained two mutations (C to U at position 122 and A to G at position 298), both of which have been shown by mutagenesis to lie in sequence motifs (pyrII and the domain IIIe tetraloop, respectively), which are crucial to IRES function (46, 57). Similarly, the single mutation in B23 (U to C at position 259) falls within the domain IIId loop E motif, a highly conserved region, in which mutations are deleterious to IRES function (20). The A204, A243 mutation, present in 25% of the brain clones (B5), had no effect on IRES function in the cell lysate system. Similarly, two minor serum sequences (S4 and S8) with mutations at position 204 (C to U in S4) and within or near the domain IIIb internal loop (A to G at position 179 and G to A at position 217 in S8) and both loci of potential functional importance, showed no significant reduction of IRES function.

In patient B, there were also marked reductions in IRES activity in two brain-derived sequences compared to the consensus sequence (B15 = 46%, and B32 = 32% [$P < 0.001$]). Both of these sequences contained mutations within domain IV. In B15 there were two mutations at the 3′ end of the pseudoknot (G to A at position 331 and U to C at position 336), and in B32 there was a single mutation immediately after the AUG start codon (A to G at position 345, leading to a serine-to-glycine substitution). There was no alteration of IRES activity in the third brain-derived sequence (B12), where there were two synonymous mutations in the core-coding sequence.

IRES translational activity in cell lines. In order to confirm our in vitro findings in conditions that more closely approximated natural polyprotein translation, and to test the hypothesis that brain-derived IRES sequences have different activities in microglia and liver cells, the constructs were tested in intact HuH7 cells of hepatocellular carcinoma origin and in CHME3 cells of fetal microglial origin (19). The translational efficiencies in these experiments broadly mirrored the results obtained in cell lysates, with some notable differences (Fig. 6).

In patient A, the brain-derived A204, A243 sequence (B5) showed reduced translational activity in CHME3 cells but preserved function in HuH7 cells, as was seen in the lysates. Similarly, the brain-derived sequence B20 showed reduced translational activity in CHME3 cells but enhanced activity in HuH7 cells. This sequence again had a single mutation within domain IV, just upstream from the AUG codon (C to U at position 340) and a synonymous mutation within the core-coding sequence. In both of these cases, the differences were small (B20 CHME3/HuH7 translational activity = 68%; B5 CHME3/HuH7 translational activity = 83%), but they were statistically significant. Brain-derived sequences B4 and B23 showed significant reductions in translational activity, which were to a similar degree in both cell lines. The serum-derived sequences all had preserved translational activity in both cell lines.

In patient B, the brain-derived sequences B15 and B32 displayed significantly reduced translational efficiencies in both cell lines, although their relative activities were reversed compared to the cell lysate results. Sequence B12, which had two synonymous mutations in the 5′ end of the core-coding region (A to G at position 368 and T to C at position 392) but a consensus noncoding sequence, displayed slightly reduced

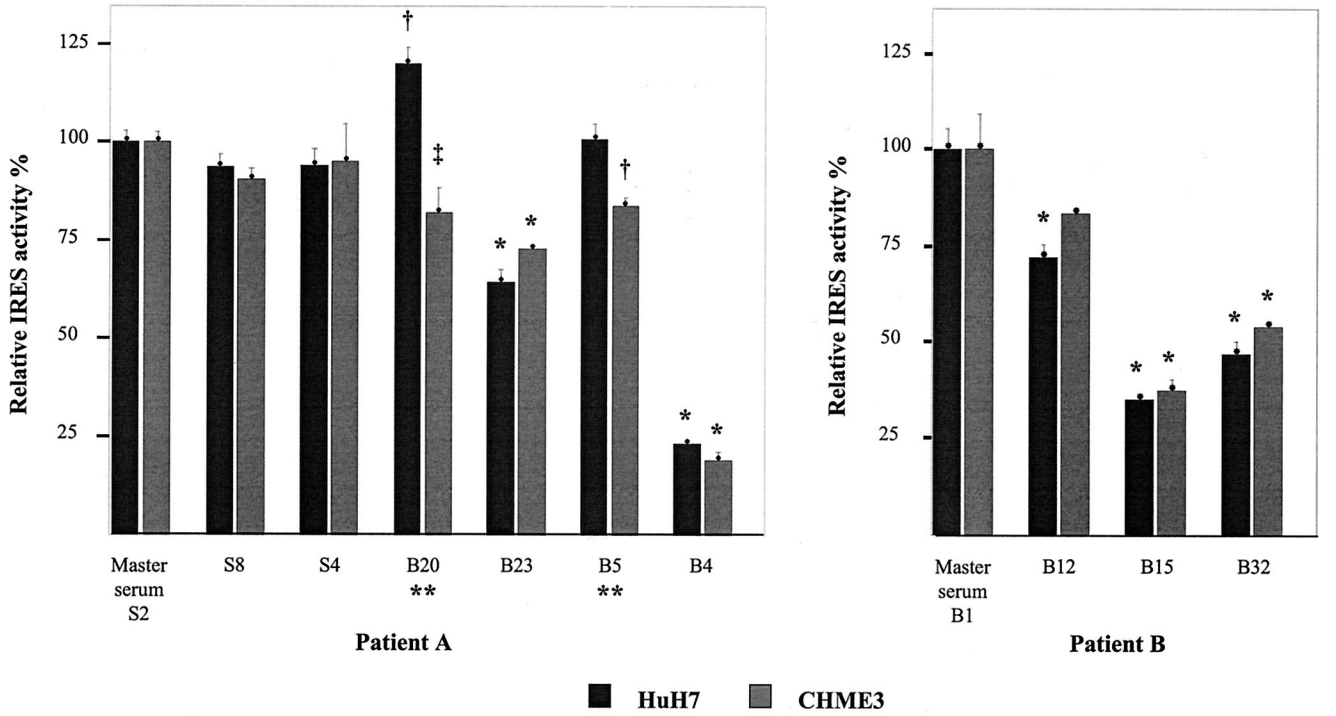

FIG. 6. Translation efficiencies of HCV IRES variants from patients A and B in HuH7 and CHME3 cell lines. Translation efficiencies are shown relative to the master serum variant. The results shown represent the means obtained from at least three experiments for each IRES ± standard errors. Differences were tested with analysis of variance and a Bonferroni correction. The following *P* values refer to comparisons with the master serum sequence: *, $P < 0.001$; †, $P < 0.025$; ‡, $P = 0.05$. There were statistical differences in translation efficiency in HuH7 and CHME3 cells for IRES variants B20 and B5 in patient A (**, $P = 0.005$).

IRES function in cell lines but preserved function in the cell lysates.

DISCUSSION

The present study was undertaken to seek evidence of HCV replication within the CNS and to determine whether variability occurring in HCV IRES sequences could confer a functional advantage in microglia, the putative cellular locus of infection within the brain.

Our approach relies upon the high fidelity of the DNA polymerase employed in PCR. The possibility that the observed sequence variability resulted from artifactual nucleotide misincorporations during reverse transcription-PCR, particularly in samples with a low RNA template level, was considered but is highly unlikely, for the following reasons. First, we employed a DNA polymerase mixture with proofreading capability (Expand; Roche), which showed greatest fidelity in a recent study that examined the mutation rates of a number of commercially available preparations during PCR of the HCV 5′ UTR (39). Second, the numbers of mutations in this study exceed, by severalfold, the expected numbers calculated according to the error rates both given by the manufacturer and determined experimentally for the HCV 5′ UTR (39). Third, we analyzed an appropriate number of clones (13), and the same mutations were sometimes seen in more than one clone from the same compartment or in two different compartments (i.e., resulting from two separate PCRs) or, in the case of the A204, A243 mutations in patient A, have been previously reported. Finally, with the exception of the brain quasispecies in patient A, where the A204, A243 mutations were detected, Pn was broadly equivalent in the brain, liver, and lymph quasispecies, arguing against an excess of artifactual misincorporations due to a possible low template copy number in extrahepatic sites.

In this study we report original observations further supporting the concept of HCV replication within the CNS. The quasispecies analysis shows evidence of tissue compartmentalization of HCV variants in brain and lymph node samples, with evidence of phylogenetic and phenetic clustering in all cases except the IRES clones in patient B. The consensus sequences were the same in each compartment, as expected, since serum-derived virus could not be removed from the tissue samples prior to RNA extraction. The different proportions of unique brain-derived sequences in the IRES and E2/HVR1 quasispecies may be explained by variation in the amount of contaminating serum-derived virus or by the selective adsorption of serum-derived E2/HVR1 variants to tissue samples (33). The high probability of serum contamination of tissue samples limits the conclusions that can be drawn from the complexity and Sn calculations. Nevertheless, 55 and 24% of the brain IRES sequences (in patients A and B, respectively) were not represented in serum, suggesting tissue derivation, as opposed to serum contamination, at least for patient A, where there was phylogenetic and phenetic compartmentalization of some of these sequences. Similarly, the presence of phylogentically and

phenetically distinct E2/HVR1 variants in the brains in both patients (B6 and B23 in patient A; B5, B9, and B11 in patient B) suggests tissue derivation. The close phylogenetic relationship between B6, B23, and N10 in patient A raises the possibility that these sequences may confer tropism to both a brain and a lymphoid compartment or, perhaps more likely, are evidence of an historical latent infection of these compartments.

Of most interest, the 5′ UTR A204, A243 mutation was detected in 25% of brain clones in patient A and was not seen in the other compartments. This mutation has consistently been associated with lymphoid compartment infection, in association with a G-to-A mutation at position 107. Long-term cultures of HPBMa and Daudi cells, inoculated with wild-type virus not containing A107, A204, and A243, selected out this variant as a dominant variant at 193 and 308 days postinoculation (41). Subsequently, these mutations have been detected in human clinical specimens, with the demonstration of the A204 mutation in PBMCs (33) and monocytes/macrophages (30) and of the A107, A204, A243 mutation in monocyte-derived dendritic cells (27). Furthermore, Radkowski and colleagues recently detected A204, A243 in the positive and negative strands isolated from the cerebellum of one patient when it was absent from serum (48). The same group reported the A107, A204, A243 mutation in cell pellets from cerebrospinal fluid obtained from human immunodeficiency virus-positive patients with meningitis or cerebral toxoplasmosis (29). In the last case it seems likely that these sequences were derived from PBMCs that had crossed a damaged blood-brain barrier. It is important to note that A204, A243 is commonly found in genotype 1a, but not genotype 1b (8). It is not presently clear whether the isolation of A204, A243 from extrahepatic sites in patients infected with genotype 1b virus in the serum represents mixed-genotype infection or a true A204, A243 mutation of genotype 1b.

A further novel aspect to this study was the testing of translational activity of brain- and serum-derived IRES variants. The finding that translational activity was generally reduced in the unique brain-derived but not serum-derived or common IRES sequences may reflect viral adaptation to a state of latency in extrahepatic sites, as recently proposed by Laporte and colleagues (27). According to this hypothesis, low translational efficiency might result in reduced synthesis of viral proteins and reduced immune destruction of infected cells, favoring viral persistence. Our findings that all but one of the brain-derived IRES sequences showed reduced activity in CHME3 cells and that IRES activity was preserved in HuH7 cells in two of these constructs (B5 and B20) suggest that IRES sequences may evolve to favor latency in the brain with preserved fitness in the liver. In the present study, the A204, A243 mutation (B5) behaved in this way. This parallels the recent observation of reduced translational activity of a construct with this mutation in dendritic cells (27). However, in the same study, a similar reduction of IRES activity was seen in HuH7 and HepG2 cells, which was not seen in our study. This may be due to differences in the construction of the dicistronic reporter vectors used. The DCV-IRES constructs included the core-coding sequence as far as nucleotide 414, whereas in the dendritic cell experiments the core-coding segment ended at nucleotide 371. There are known long-range RNA-RNA interactions between the core-coding sequences and nucleotides 24 to 39 of the 5′ UTR, although the implicated core-coding sequences are thought to be downstream of nucleotide 414 (22). In addition, DCV contained an A-to-G mutation at position 34, which was introduced by the universal primer used for synthesis of the DCV-IRES constructs. Positions 34 and 35 have an important regulatory role in IRES activity, again through an interaction with the core-coding sequence from nucleotide 408 to 929 (18). A final explanation is that there were differences in the expression of cellular factors, which affect cap-independent translation in the different cell lines that were used.

In this study we have not examined IRES activities of the liver and lymph node minority sequences. In patient A, it is interesting that the mutations segregate along the IRES, with the brain sequence mutations all found in domains III and IV, specifically within the pyrII motif, the domain IIIe tetraloop, and the domain IIId loop E motif, which are crucial to IRES function (20, 46, 57), in addition to the A204, A243 mutation (Fig. 7). In contrast, liver, serum, and lymph node sequence mutations were found throughout the IRES. It is unknown what the significance of this is in terms of IRES activity. However, it is likely to be of considerable interest in determining whether a similar viral strategy of reduced translation efficiency might favor latency in the reticuloendothelial system and within compartments inside the liver.

It might be expected that at times when HCV polyprotein translation is reduced, replication of viral RNA might be increased as both processes compete for positive-strand RNA (63). It has been suggested that during replication, mutations within the structural coding regions accumulate, because they do not undergo selection during this phase (52). Selection of structural genes by the immune system occurs only after protein translation. Therefore, in cells with lower levels of HCV translation, one might expect increases in structural gene nucleotide complexity and diversity. In patient A, this appears to be the case for the E2/HVR1 sequences, with greater Pn and mean within-sample distances in brain and lymph node compared to liver and serum. Furthermore, both an insertion resulting in a frameshift and a stop codon mutation are found in the brain and lymph node sequences, consistent with absent or reduced immune selection. In patient B, Pn and the mean within sample distances are equivalent in brain and liver, but greater than in serum, as the model predicts.

Our observations and those of Radkowski and colleagues provide evidence that the CNS is a site of HCV replication (48), which probably occurs at a considerably lower level than in the liver. Together with other potential sanctuary sites, such as dendritic cells (27), the brain may allow low-level viral replication to occur without eliciting an immune response sufficient to terminate it. The pattern of relapsing lobular hepatitis seen in HCV infection may represent a repeated cycle of immune lysis of infected hepatocytes, followed by repopulation by virus from low-replication sites. Similarly, it is possible that the relapse seen after initially successful antiviral treatment may be a result of persistent low-level replication in sites such as the brain and dendritic cells, which may be less responsive to therapy. In this study, the data are more compelling for patient A (genotype 1) than for patient B (genotype 3), raising the possibility that genotypic variation in extrahepatic replication

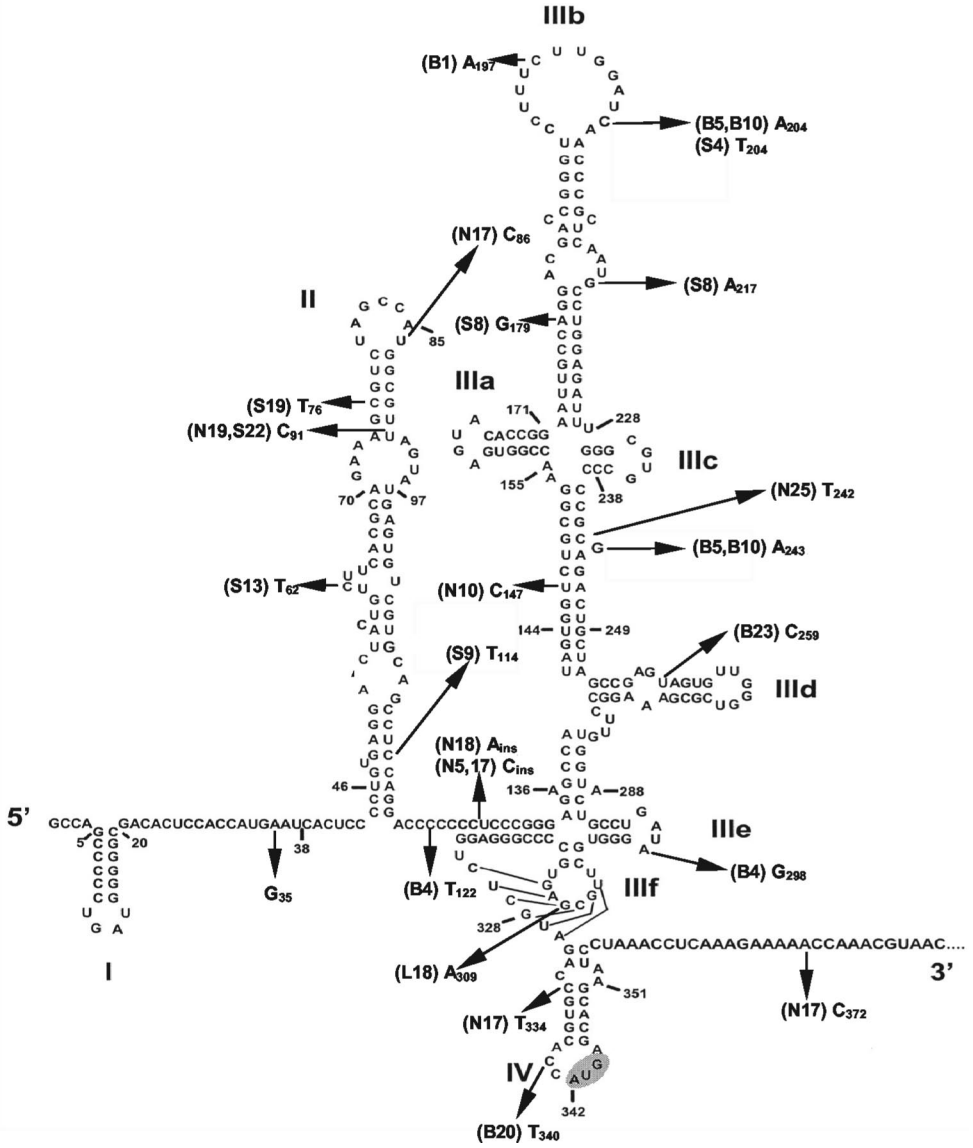

FIG. 7. Sequence and secondary structure of HCV IRES RNA (nucleotides 1 to 383, genotype 1b), showing the positions of mutations detected in patient A. Domains are numbered as described by Brown et al. (5). Sequence identifiers are shown in parentheses. Figure is modified from Honda et al. (18).

may underlie the differences in response to treatment. However, further studies are required both to examine this possibility and to establish the frequency of CNS infection by HCV.

We have previously speculated that low-level infection of the CNS by HCV might underlie the neuropsychological symptoms and cognitive impairment in chronic HCV infection (9–12, 55) that have been described by our group and others (15, 23). A model of low-level immune activation within the brain, secondary to HCV infection, possibly introduced to the CNS by infected monocytes, has been described extensively elsewhere (9, 10, 12). This model remains to be proven. However, the emerging similarities between quasispecies sequences in brain and dendritic cells, the possibility of latency in these sites, and the functional sequelae may lead to a model that explains a number of unresolved issues, in terms of both clinical symptoms and viral persistence.

ACKNOWLEDGMENTS

The European Association for the Study of the Liver supported Daniel M. Forton.

We are grateful to N. Janabi for providing us with the CHME3 cells and to Robert Goldin, Emanuele Durante-Mangoni, and the staff of the Hepatology Section at St. Mary's Hospital for their assistance.

REFERENCES

1. **Afonso, A. M., J. Jiang, F. Penin, C. Tareau, D. Samuel, M. A. Petit, H. Bismuth, E. Dussaix, and C. Feray.** 1999. Nonrandom distribution of hepatitis C virus quasispecies in plasma and peripheral blood mononuclear cell subsets. J. Virol. **73:**9213–9221.
2. **Alter, M. J., H. S. Margolis, K. Krawczynski, F. N. Judson, A. Mares, W. J. Alexander, P. Y. Hu, J. K. Miller, M. A. Gerber, R. E. Sampliner, et al.** 1992.

The natural history of community-acquired hepatitis C in the United States. N. Engl. J. Med. **327:**1899–1905.
3. **Bouffard, P., P. H. Hayashi, R. Acevedo, N. Levy, and J. B. Zeldis.** 1992. Hepatitis C virus is detected in a monocyte/macrophage subpopulation of peripheral blood mononuclear cells of infected patients. J. Infect. Dis. **166:** 1276–1280.
4. **Bronowicki, J. P., M. A. Loriot, V. Thiers, Y. Grignon, A. L. Zignego, and C. Brechot.** 1998. Hepatitis C virus persistence in human hematopoietic cells injected into SCID mice. Hepatology **28:**211–218.
5. **Brown, E. A., H. Zhang, L. H. Ping, and S. M. Lemon.** 1992. Secondary structure of the 5′ nontranslated regions of hepatitis C virus and pestivirus genomic RNAs. Nucleic Acids Res. **20:**5041–5045.
6. **Cabot, B., M. Martell, J. I. Esteban, S. Sauleda, T. Otero, R. Esteban, J. Guardia, and J. Gomez.** 2000. Nucleotide and amino acid complexity of hepatitis C virus quasispecies in serum and liver. J. Virol. **74:**805–811.
7. **Choo, Q. L., G. Kuo, A. J. Weiner, L. R. Overby, D. W. Bradley, and M. Houghton.** 1989. Isolation of a cDNA clone derived from a blood-borne non-A, non-B viral hepatitis genome. Science **244:**359–362.
8. **Collier, A. J., S. Tang, and R. M. Elliott.** 1998. Translation efficiencies of the 5′ untranslated region from representatives of the six major genotypes of hepatitis C virus using a novel bicistronic reporter assay system. J. Gen. Virol. **79:**2359–2366.
9. **Forton, D. M., J. M. Allsop, J. Main, G. R. Foster, H. C. Thomas, and S. D. Taylor-Robinson.** 2001. Evidence for a cerebral effect of the hepatitis C virus. Lancet **358:**38–39.
10. **Forton, D. M., S. D. Taylor-Robinson, and H. C. Thomas.** 2002. Reduced quality of life in hepatitis C—is it all in the head? J. Hepatol. **36:**435–438.
11. **Forton, D. M., S. D. Taylor-Robinson, and H. C. Thomas.** 2003. Cerebral dysfunction in chronic hepatitis C infection. J. Viral Hepat. **10:**81–86.
12. **Forton, D. M., H. C. Thomas, C. A. Murphy, J. M. Allsop, G. R. Foster, J. Main, K. A. Wesnes, and S. D. Taylor-Robinson.** 2002. Hepatitis C and cognitive impairment in a cohort of patients with mild liver disease. Hepatology **35:**433–439.
13. **Gomez, J., M. Martell, J. Quer, B. Cabot, and J. I. Esteban.** 1999. Hepatitis C viral quasispecies. J. Viral Hepat. **6:**3–16.
14. **Gowans, E. J.** 2000. Distribution of markers of hepatitis C virus infection throughout the body. Semin. Liver Dis. **20:**85–102.
15. **Hilsabeck, R. C., W. Perry, and T. I. Hassanein.** 2002. Neuropsychological impairment in patients with chronic hepatitis C. Hepatology **35:**440–446.
16. **Honda, M., M. R. Beard, L. H. Ping, and S. M. Lemon.** 1999. A phylogenetically conserved stem-loop structure at the 5′ border of the internal ribosome entry site of hepatitis C virus is required for cap-independent viral translation. J. Virol. **73:**1165–1174.
17. **Honda, M., L. H. Ping, R. C. Rijnbrand, E. Amphlett, B. Clarke, D. Rowlands, and S. M. Lemon.** 1996. Structural requirements for initiation of translation by internal ribosome entry within genome-length hepatitis C virus RNA. Virology **222:**31–42.
18. **Honda, M., R. Rijnbrand, G. Abell, D. Kim, and S. M. Lemon.** 1999. Natural variation in translational activities of the 5′ nontranslated RNAs of hepatitis C virus genotypes 1a and 1b: evidence for a long-range RNA-RNA interaction outside of the internal ribosomal entry site. J. Virol. **73:**4941–4951.
19. **Janabi, N., S. Peudenier, B. Heron, K. H. Ng, and M. Tardieu.** 1995. Establishment of human microglial cell lines after transfection of primary cultures of embryonic microglial cells with the SV40 large T antigen. Neurosci. Lett. **195:**105–108.
20. **Jubin, R., N. E. Vantuno, J. S. Kieft, M. G. Murray, J. A. Doudna, J. Y. Lau, and B. M. Baroudy.** 2000. Hepatitis C virus internal ribosome entry site (IRES) stem loop IIId contains a phylogenetically conserved GGG triplet essential for translation and IRES folding. J. Virol. **74:**10430–10437.
21. **Kao, J. H., P. J. Chen, M. Y. Lai, T. H. Wang, and D. S. Chen.** 1997. Positive and negative strand of hepatitis C virus RNA sequences in peripheral blood mononuclear cells in patients with chronic hepatitis C: no correlation with viral genotypes 1b, 2a, and 2b. J. Med. Virol. **52:**270–274.
22. **Kim, Y. K., S. H. Lee, C. S. Kim, S. K. Seol, and S. K. Jang.** 2003. Long-range RNA-RNA interaction between the 5′ nontranslated region and the core-coding sequences of hepatitis C virus modulates the IRES-dependent translation. RNA **9:**599–606.
23. **Kramer, L., E. Bauer, G. Funk, H. Hofer, W. Jessner, P. Steindl-Munda, F. Wrba, C. Madl, A. Gangl, and P. Ferenci.** 2002. Subclinical impairment of brain function in chronic hepatitis C infection. J. Hepatol. **37:**349–354.
24. **Kumar, S., K. Tamura, I. B. Jakobsen, and M. Nei.** 2001. MEGA2: molecular evolutionary genetics analysis software. Bioinformatics **17:**1244–1245.
25. **La Monica, N., and V. R. Racaniello.** 1989. Differences in replication of attenuated and neurovirulent polioviruses in human neuroblastoma cell line SH-SY5Y. J. Virol. **63:**2357–2360.
26. **Lanford, R. E., D. Chavez, F. V. Chisari, and C. Sureau.** 1995. Lack of detection of negative-strand hepatitis C virus RNA in peripheral blood mononuclear cells and other extrahepatic tissues by the highly strand-specific rTth reverse transcriptase PCR. J. Virol. **69:**8079–8083.
27. **Laporte, J., C. Bain, P. Maurel, G. Inchauspe, H. Agut, and A. Cahour.** 2003. Differential distribution and internal translation efficiency of hepatitis C virus quasispecies present in dendritic and liver cells. Blood **101:**52–57.
28. **Laporte, J., I. Malet, T. Andrieu, V. Thibault, J. J. Toulme, C. Wychowski, J. M. Pawlotsky, J. M. Huraux, H. Agut, and A. Cahour.** 2000. Comparative analysis of translation efficiencies of hepatitis C virus 5′ untranslated regions among intraindividual quasispecies present in chronic infection: opposite behaviors depending on cell type. J. Virol. **74:**10827–10833.
29. **Laskus, T., M. Radkowski, A. Bednarska, J. Wilkinson, D. Adair, M. Nowicki, G. B. Nikolopoulou, H. Vargas, and J. Rakela.** 2002. Detection and analysis of hepatitis C virus sequences in cerebrospinal fluid. J. Virol. **76:** 10064–10068.
30. **Laskus, T., M. Radkowski, A. Piasek, M. Nowicki, A. Horban, J. Cianciara, and J. Rakela.** 2000. Hepatitis C virus in lymphoid cells of patients coinfected with human immunodeficiency virus type 1: evidence of active replication in monocytes/macrophages and lymphocytes. J. Infect. Dis. **181:**442–448.
31. **Laskus, T., M. Radkowski, L. F. Wang, J. Cianciara, H. Vargas, and J. Rakela.** 1997. Hepatitis C virus negative strand RNA is not detected in peripheral blood mononuclear cells and viral sequences are identical to those in serum: a case against extrahepatic replication. J. Gen. Virol. **78:** 2747–2750.
32. **Laskus, T., M. Radkowski, L. F. Wang, S. J. Jang, H. Vargas, and J. Rakela.** 1998. Hepatitis C virus quasispecies in patients infected with HIV-1: correlation with extrahepatic viral replication. Virology **248:**164–171.
33. **Laskus, T., M. Radkowski, L. F. Wang, M. Nowicki, and J. Rakela.** 2000. Uneven distribution of hepatitis C virus quasispecies in tissues from subjects with end-stage liver disease: confounding effect of viral adsorption and mounting evidence for the presence of low-level extrahepatic replication. J. Virol. **74:**1014–1017.
34. **Laskus, T., M. Radkowski, L. F. Wang, H. Vargas, and J. Rakela.** 1998. Search for hepatitis C virus extrahepatic replication sites in patients with acquired immunodeficiency syndrome: specific detection of negative-strand viral RNA in various tissues. Hepatology **28:**1398–1401.
35. **Lerat, H., F. Berby, M. A. Trabaud, O. Vidalin, M. Major, C. Trepo, and G. Inchauspe.** 1996. Specific detection of hepatitis C virus minus strand RNA in hematopoietic cells. J. Clin. Investig. **97:**845–851.
36. **Lerat, H., S. Rumin, F. Habersetzer, F. Berby, M. A. Trabaud, C. Trepo, and G. Inchauspe.** 1998. In vivo tropism of hepatitis C virus genomic sequences in hematopoietic cells: influence of viral load, viral genotype, and cell phenotype. Blood **91:**3841–3849.
37. **Lerat, H., Y. K. Shimizu, and S. M. Lemon.** 2000. Cell type-specific enhancement of hepatitis C virus internal ribosome entry site-directed translation due to 5′ nontranslated region substitutions selected during passage of virus in lymphoblastoid cells. J. Virol. **74:**7024–7031.
38. **Madejon, A., M. L. Manzano, C. Arocena, I. Castillo, and V. Carreno.** 2000. Effects of delayed freezing of liver biopsies on the detection of hepatitis C virus RNA strands. J. Hepatol. **32:**1019–1025.
39. **Malet, I., M. Belnard, H. Agut, and A. Cahour.** 2003. From RNA to quasispecies: a DNA polymerase with proofreading activity is highly recommended for accurate assessment of viral diversity. J. Virol. Methods **109:** 161–170.
40. **McGuinness, P. H., G. A. Bishop, G. W. McCaughan, R. Trowbridge, and E. J. Gowans.** 1994. False detection of negative-strand hepatitis C virus RNA. Lancet **343:**551–552.
41. **Nakajima, N., M. Hijikata, H. Yoshikura, and Y. K. Shimizu.** 1996. Characterization of long-term cultures of hepatitis C virus. J. Virol. **70:**3325–3329.
42. **Navas, S., J. Martin, J. A. Quiroga, I. Castillo, and V. Carreno.** 1998. Genetic diversity and tissue compartmentalization of the hepatitis C virus genome in blood mononuclear cells, liver, and serum from chronic hepatitis C patients. J. Virol. **72:**1640–1646.
43. **Negro, F., and M. Levrero.** 1998. Does the hepatitis C virus replicate in cells of the hematopoietic lineage? Hepatology **28:**261–264.
44. **Okuda, M., K. Hino, M. Korenaga, Y. Yamaguchi, Y. Katoh, and K. Okita.** 1999. Differences in hypervariable region 1 quasispecies of hepatitis C virus in human serum, peripheral blood mononuclear cells, and liver. Hepatology **29:**217–222.
45. **Poss, M., A. G. Rodrigo, J. J. Gosink, G. H. Learn, P. D. de Vange, H. L. Martin, Jr., J. Bwayo, J. K. Kreiss, and J. Overbaugh.** 1998. Evolution of envelope sequences from the genital tract and peripheral blood of women infected with clade A human immunodeficiency virus type 1. J. Virol. **72:** 8240–8251.
46. **Psaridi, L., U. Georgopoulou, A. Varaklioti, and P. Mavromara.** 1999. Mutational analysis of a conserved tetraloop in the 5′ untranslated region of hepatitis C virus identifies a novel RNA element essential for the internal ribosome entry site function. FEBS Lett. **453:**49–53.
47. **Quadri, R., L. Rubbia-Brandt, K. Abid, and F. Negro.** 2001. Detection of the negative-strand hepatitis C virus RNA in tissues: implications for pathogenesis. Antivir. Res. **52:**161–171.
48. **Radkowski, M., J. Wilkinson, M. Nowicki, D. Adair, H. Vargas, C. Ingui, J. Rakela, and T. Laskus.** 2002. Search for hepatitis C virus negative-strand RNA sequences and analysis of viral sequences in the central nervous system: evidence of replication. J. Virol. **76:**600–608.
49. **Sanchez, I. J., and B. H. Ruiz.** 1996. A single nucleotide change in the E

protein gene of dengue virus 2 Mexican strain affects neurovirulence in mice. J. Gen. Virol. **77:**2541–2545.
50. **Shimizu, Y. K., H. Igarashi, T. Kanematu, K. Fujiwara, D. C. Wong, R. H. Purcell, and H. Yoshikura.** 1997. Sequence analysis of the hepatitis C virus genome recovered from serum, liver, and peripheral blood mononuclear cells of infected chimpanzees. J. Virol. **71:**5769–5773.
51. **Soler, M., M. Pellerin, C. E. Malnou, D. Dhumeaux, K. M. Kean, and J. M. Pawlotsky.** 2002. Quasispecies heterogeneity and constraints on the evolution of the 5′ noncoding region of hepatitis C virus (HCV): relationship with HCV resistance to interferon-alpha therapy. Virology **298:**160–173.
52. **Stumpf, M. P., and N. Zitzmann.** 2001. RNA replication kinetics, genetic polymorphism and selection in the case of the hepatitis C virus. Proc. R. Soc. Lond. B **268:**1993–1999.
53. **Sumiyoshi, H., G. H. Tignor, and R. E. Shope.** 1995. Characterization of a highly attenuated Japanese encephalitis virus generated from molecularly cloned cDNA. J. Infect. Dis. **171:**1144–1151.
54. **Takyar, S. T., D. Li, Y. Wang, R. Trowbridge, and E. J. Gowans.** 2000. Specific detection of minus-strand hepatitis C virus RNA by reverse-transcription polymerase chain reaction on polyA(+)-purified RNA. Hepatology **32:**382–387.
55. **Thomas, H. C., M. E. Torok, D. M. Forton, and S. D. Taylor-Robinson.** 1999. Possible mechanisms of action and reasons for failure of antiviral therapy in chronic hepatitis C. J. Hepatol. **31**(Suppl. 1)**:**152–159.
56. **Tsukiyama-Kohara, K., N. Iizuka, M. Kohara, and A. Nomoto.** 1992. Internal ribosome entry site within hepatitis C virus RNA. J. Virol. **66:**1476–1483.
57. **Varaklioti, A., U. Georgopoulou, A. Kakkanas, L. Psaridi, M. Serwe, W. H. Caselmann, and P. Mavromara.** 1998. Mutational analysis of two unstructured domains of the 5′ untranslated region of HCV RNA. Biochem. Biophys. Res. Commun. **253:**678–685.
58. **Wang, C., S. Y. Le, N. Ali, and A. Siddiqui.** 1995. An RNA pseudoknot is an essential structural element of the internal ribosome entry site located within the hepatitis C virus 5′ noncoding region. RNA **1:**526–537.
59. **Wang, J. T., J. C. Sheu, J. T. Lin, T. H. Wang, and D. S. Chen.** 1992. Detection of replicative form of hepatitis C virus RNA in peripheral blood mononuclear cells. J. Infect. Dis. **166:**1167–1169.
60. **Westaway, E. G.** 1987. Flavivirus replication strategy. Adv. Virus Res. **33:** 45–90.
61. **Young, K. C., T. T. Chang, T. C. Liou, and H. L. Wu.** 1993. Detection of hepatitis C virus RNA in peripheral blood mononuclear cells and in saliva. J. Med. Virol. **41:**55–60.
62. **Zhang, J., O. Yamada, T. Ito, M. Akiyama, Y. Hashimoto, H. Yoshida, R. Makino, A. Masago, H. Uemura, and H. Araki.** 1999. A single nucleotide insertion in the 5′-untranslated region of hepatitis C virus leads to enhanced cap-independent translation. Virology **261:**263–270.
63. **Zhang, J., O. Yamada, H. Yoshida, T. Iwai, and H. Araki.** 2002. Autogenous translational inhibition of core protein: implication for switch from translation to RNA replication in hepatitis C virus. Virology **293:**141–150.
64. **Zignego, A. L., M. De Carli, M. Monti, G. Careccia, G. La Villa, C. Giannini, M. M. D'Elios, G. Del Prete, and P. Gentilini.** 1995. Hepatitis C virus infection of mononuclear cells from peripheral blood and liver infiltrates in chronically infected patients. J. Med. Virol. **47:**58–64.